Preprints of the 21st IFAC World Congress (Virtual)
Berlin, Germany, July 12-17, 2020

LPV Based Control of Glucose Concentration in Type 2 Diabetes ⋆

Deividas Eringis * **Peter Aurelius Munk** *
Benjamin Keldberg Andersen * **Rahul Sylvester Suresh** *
John Leth *

* *Automation & Control, Aalborg University, Denmark (e-mail: (dering15, pmunk15, bkan15, rsures18)@student.aau.dk, jjl@es.aau.dk).*

Abstract: This paper investigates continuous-time LPV dynamic-output feedback for controlling a type 2 diabetes patients' fasting glucose concentration. To emulate a real life scenario, the input and measurement were specified only once per day, and biological variance was introduced. The results were evaluated by examining the settling time, variance after settling, and the violation of the nominal fasting glucose concentration range of $4-5$ $[mmol/l]$. The LPV dynamic-output feedback controller was compared to a simple rule based titration algorithm and a PI controller tuned by LPV methods. The LPV dynamic-output feedback controller, proved to deliver better results, in particular for the transient period.

Keywords: Type 2 Diabetes, LPV control, Diabetes.

1. INTRODUCTION

Diabetes mellitus, hereafter, referred to as diabetes, is increasingly becoming a global burden. As one of the four non-communicable diseases (NCD), diabetes is accountable for 1.6 million of 41 million yearly NCD related premature deaths. The deaths before the age of 70 are defined as premature deaths. Diabetes is a chronic, progressive disease. However, a series of interventions can improve the health of patients, so they live longer with a higher quality of life (International Diabetes Federation, 2017).

The most prevalent types of diabetes are type 1 diabetes (T1D) accounting for 9% and type 2 diabetes (T2D) accounting for 89%, see (International Diabetes Federation, 2017). In 2017 a total of 425 million in the age group of adults from 20 to 79 years was estimated to have diabetes. This number is estimated to increase to 629 million by 2045 (International Diabetes Federation, 2017).

T2D patients monitor their glucose concentration with a glucometer, in order to be in the nominal range, 4 to 7 [mmol/l](Diabetes.co.uk, 2019) and to avoid high concentration leading to hyperglycemia, or dangerously low concentration leading to hypoglycemia.

Table 1 shows the different concentrations of blood glucose and the associated risk levels. To regulate the glucose concentration, insulin is injected.

The Sample Treat-to-Target Algorithm (Swigert, 2014) is a simple algorithm for basal insulin titration, where one or more daily fasting glucose (FG) measurements are used to determine a daily dose for insulin injection. Based on a target FG level the insulin dose is increased daily until the target FG level is reached. The dose is lowered immediately if FG measurements are significantly lower than the target is observed.

Table 1. Mean fasting glucose

Level	mmol/l	Risk
Dangerously high	17.4	Very high
High	[11,15.6]	High
Borderline	[7,10]	Medium
Normal	[4,6]	No risk
Low	3.9	Medium
Dangerously low	2.8	High

Linear parameter-varying (LPV) based control algorithms have previously been investigated for use in controlling the blood glucose concentration in diabetes mellitus patients. However, the use of such algorithms have exclusively been employed for T1D patients.

The identification of an LPV model describing the glucose-insulin dynamics of the T1D patient is investigated in (Cer, 2012). It is concluded that the identified model provides a satisfactory description of the dynamics.

LPV based control for glucose concentration was investigated in (Colmegna and Peña, 2014). The paper tests the controller on 10 simulated adults from a T1D designed simulator to analyse the closed-loop performance, the tests also includes unannounced meals. The authors concluded that stability and robustness is guaranteed based on Lyapunov theory, and with the use of *on-line* tuning they reduced the risk of having hypoglycemic and hyperglycemic events.

A switched LPV controller with multiple regions related to hypo-, hyper-, and euglycemia situations was proposed in (Colmegna et al., 2016). The model, the controller is based on, is tuned with *a priori* patient information. Additionally an estimator is used to predict perturbations.

⋆ This work was funded by the IFD Grand solution project ADAPT-T2D, project number 9068-00056B.

The modelling and discretization of a T1D patient model in the LPV framework is explored in (Eigner et al., 2018). Three different LPV discretization methods, and two Jacobian based discretization methods are introduced, analysed and proven by RMSE based error assessment.

In (Aradóttir et al., 2017), a physiological model of T1D is augmented with endogenous insulin production in T2D in order to obtain a model for simulating FG for T2D patients. The effect of dose guidance and adherence to injection is investigated and compared to results from clinical trials. It is concluded that the model is sufficient to simulate FG concentrations in a clinical trial. In Aradóttir et al. (2018), the model is modified to allow for identification of parameters. The identifiability of parameters is investigated, and parameter estimation from simulated and clinical data is performed.

The aim of this paper is to show that linear parameter-varying based control methods are applicable for controlling the glucose concentrations in T2D patients, and able to manage the transient period with good performance. Indeed it is shown that dynamic-output feedback in an LPV setting give better robust performance when compared to the rule-based titration algorithm described in (Aradóttir et al., 2017) and standard PI control (see Table 5 and 6).

The rest of this paper proceeds as follows. Section 2 introduces a physiological model for simulating T2D patients using long-acting insulin. Simulation of glucose consumption, insulin injection and biological variability is also presented. Lastly, an LPV representation of the physiological model for controller design is explored. In section 3, an LPV based Dynamic-Output Feedback controller is derived. In section 4, a comparison of results between the proposed LPV control algorithm and the rule-based algorithm is presented. Lastly, section 5 concludes on the methods and results explored.

The numerical results of this paper is obtained using YALMIP (Löfberg, 2004) as LMI parser, and MOSEK as solver.

2. THE INVESTIGATED MODEL

This section details the model describing the dynamics of glucose concentration and long-acting insulin in type 2 diabetes patients. Furthermore, the decisions made in regards to the design of controllers for the system are presented.

2.1 Physiological Model

The physiological model describing the long-acting insulin and glucose concentration in type 2 diabetes patients is as described in (Aradóttir et al., 2018):

$$\dot{x}_1 = \frac{1}{p_1}u - \frac{1}{p_1}x_1 \tag{1a}$$

$$\dot{x}_2 = \frac{1}{p_1}x_1 - \frac{1}{p_1}x_2 \tag{1b}$$

$$\dot{x}_3 = p_3(x_2 + p_7 x_4) - p_3 x_3 \tag{1c}$$

$$\dot{x}_4 = -(p_5 + p_4 x_3)x_4 + p_6 + R_A \tag{1d}$$

with u [U/day] (1U = 34.7 μg) the exogenous insulin from injections, $\frac{x_1}{p_2}$ [U/l] and $\frac{x_2}{p_2}$ [U/l] the insulin concentration in subcutaneous and plasma respectively, $\frac{x_3 p_4}{p_2}$ [1/day] the insulin effect on glucose, and x_4 [mmol/l] the continuous glucose concentration in plasma. The parameters of the model (1) are:

- p_1 is a time constant of the insulin travelling between subcutaneous and plasma and is chosen to fit the action profile of the long-action insulin $[day]$;
- p_2 is a gain describing insulin clearance $[l/day]$;
- p_3 is the time constant describing the delay in insulin action following increased plasma insulin concentration $[1/day]$;
- p_4 is the gain describing insulin sensitivity $[1/U]$;
- p_5 is the inverse time constant describing the effect of insulin to eliminate glucose from plasma $[1/day]$;
- p_6 is the constant describing the rate of endogenous glucose production $[mmol/l \cdot day]$;
- p_7 describes the endogenous insulin production and interpreted as the sensitivity of the the insulin producing cells in the pancreas which is assumed to be increasing linearly with fasting glucose concentration $[U \cdot l/mmol \cdot day]$;
- p_v is the distribution volume of the blood glucose $[l]$.
- $R_A = \frac{D_2}{p_v p_d}$ is the rate of appearance of glucose in the plasma from the ingested food $[U/day]$.

Furthermore, the glucose from the ingested food is incorporated as described in (Aradóttir et al., 2017) using a two-compartment model represented by D_1 $[mmol]$ and D_2 $[mmol]$:

$$\dot{D}_2 = \frac{1}{p_d}D_1 - \frac{1}{p_d}D_2 \tag{2a}$$

$$\dot{D}_1 = \frac{1000}{M_{wG}}d_f - \frac{1}{p_d}D_1 \tag{2b}$$

where

- d_f is the daily glucose consumption rate (disturbance) $[g/day]$;
- p_d denotes the peak time for meal absorption $[min]$;
- $M_{wG} = 180.1559[g/mol]$ is the molar weight of glucose;

Table 2. Parameter values and distribution of the model (1).

Parameter	Value/Distribution	Modified values
p_1	0.5	
p_2	1800	
p_3	15.8	
p_4	0.44	$N(0.44, \sigma_4^2)$ $\sigma_4 \in \{0.01, 0.1\}$
p_5	3.31	
p_6	$N(96.7, 7.94^2)$	$N(96.7, 5^2)$
p_7	$N(2.52, 0.5^2)$	
p_v	22	
p_d	$ln(p_d) \sim N(\mu_d, 0.25^2)$ $\mu_d = ln\left(\frac{40}{60 \cdot 24}\right)$	$\sim N(\mu_d, 0.72^2)$ $\mu_d = ln\left(\frac{40}{60 \cdot 24}\right)$

Parameter values and distribution are shown in Table 2 with $N(\mu, \sigma^2)$ indicating normal distribution with mean μ and variance σ^2. The numerical values (in the second column) for $p_1, \ldots, p_7$ are based on (Aradóttir et al., 2018), p_v is based on Kanderian et al. (2009), and p_d is based on Hovorka et al. (2004); Wilinska et al. (2010).

2.2 Patient Simulation

The model (1)-(2) is used to generate virtual patients as follows. We will consider two cases: three varying parameters p_d, p_6 and p_7 based on the second column in Table 2, and four varying parameters p_d, p_4, p_6 and p_7 based on the third column in Table 2 with $\sigma_4 = 0.01$ and p_7 as in column two. To each of the varying parameters there will be associated three values: the 5th percentile, the mean and the 95th percentile from the parameter distribution. Thus 27 and 81 different virtual patients will be simulated. Moreover, to account for stochastic phenomena, 30 realizations of each patient will be simulated, resulting in a total of 810 and 2430 simulations per control strategy. Where each realization used a different seed for pseudo-random number generation.

The range of x_4 is determined based on the extreme values shown in Table 1, meaning $x_4 \in [0, 17.4]$. However, it is convenient when using a polytopic LPV representation to map the range of x_4 to $[0, 1]$ and to hide the bias term p_6 in the disturbance. This can be done using the following affine transformation:

$$\bar{x}_4 = \alpha x_4 \tag{3}$$

with

$$\alpha = \frac{1}{x_{4max} - x_{4min}} = \frac{1}{17.4} \tag{4}$$

implying that $\bar{x}_4 \in [0, 1]$. To hide the bias term p_6 the following transformations are used

$$\bar{x}_3 = p_3 x_3 \tag{5}$$
$$\bar{x}_4 = \alpha x_4 \tag{6}$$
$$\bar{D}_2 = \frac{\alpha}{p_v p_d} D_2 + C \tag{7}$$
$$C = \alpha p_6$$
$$\bar{D}_1 = \frac{\alpha}{p_v p_d^2} D_1 + \frac{C}{p_d} \tag{8}$$
$$\bar{d}_f = \frac{1000\alpha}{p_v p_d^2 M_{wG}} d_f + \frac{C}{p_d^2} \, . \tag{9}$$

Taking time derivatives of (5)-(9), using (1), and substituting in the definitions, yields the following model equivalent to (1)-(2):

$$\dot{x} = A_p x + B_p u + E_p d_f \tag{10}$$

with

$$x = \begin{bmatrix} x_1 & x_2 & \bar{x}_3 & \bar{x}_4 & \bar{D}_2 & \bar{D}_1 \end{bmatrix}^T \tag{11}$$

$$A_p = \begin{bmatrix} -p_1^{-1} & 0 & 0 & 0 & 0 & 0 \\ p_1^{-1} & -p_1^{-1} & 0 & 0 & 0 & 0 \\ 0 & p_3^2 & -p_3 & \frac{p_3^2 p_7}{\alpha} & 0 & 0 \\ 0 & 0 & -\bar{x}_4 \frac{p_4}{p_3} & -p_5 & 1 & 0 \\ 0 & 0 & 0 & 0 & -p_d^{-1} & 1 \\ 0 & 0 & 0 & 0 & 0 & -p_d^{-1} \end{bmatrix} \tag{12}$$

$$B_p = \begin{bmatrix} p_1^{-1} & 0 & 0 & 0 & 0 & 0 \end{bmatrix}^T \quad E_p = \begin{bmatrix} 0 & 0 & 0 & 0 & 0 & 1 \end{bmatrix}^T \, . \tag{13}$$

Note that $A_p = A_p(\bar{x}_4)$ is a function of $\bar{x}_4$ (this will be important when constructing the LPV model).

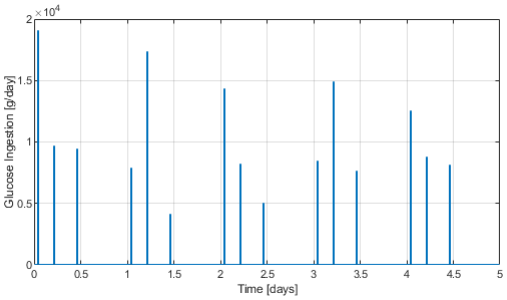

Fig. 1. Glucose ingestion for five days distributed over three daily meals

2.3 Glucose Consumption

The patient's daily glucose consumption from food sources acts as a disturbance on the system. Recommended glucose intake is $240-280$ $[g/day]$ (Bolder et al., 2009). To include variability in behaviour of patients, It is assumed that the patient will ingest between $150-400$ $[g/day]$, interpreted as $d_f \sim U(150, 400)\,[g/day]$ (uniformly distributed on [150,400]). In the simulation, the ingestion will be divided into three meals, rather than the glucose ingestion being constant throughout the day. The first and second meals, corresponding to breakfast at 8:00, and lunch at 12:00, are 10 minutes long, amounting to $1/144$ $[day]$, and the third meal, dinner at 18:00, is 20 minutes long, $1/72$ $[day]$; however with half the consumption rate pr. minute, compared with the first and second meal. The consumption is distributed such that the total consumption amount to a value in the assumed interval. This distribution of meal provide a more realistic emulation of a T2D patients daily consumption, compared to a constant rate throughout the day. In Fig. 1, the glucose consumption of a patient over 5 days is shown.

2.4 Shot Insulin Input

Insulin is given as a shot injection where the entire daily dose is given in a short interval to simulate the one daily injection that a patient would do in practice, rather than having continuous input throughout the day. FG is measured in the beginning of the day at 7am and the shot input is given at the same time. Shot insulin input on day d with injection duration $t_{in} = 2[min]$ is defined as

$$u_d(d) = \begin{cases} u_0 & \text{if } d = 0 \\ \int_{d-1}^{d} u(t)\, dt & \text{if } d \in \mathbb{Z}_{>0} \end{cases} \tag{14}$$

$$u_{sh}(d < t < d + t_{in}) = \frac{1}{t_{in}} u_d(d) \tag{15}$$

Here $u_d(d)[U]$ is the insulin dose injected on day d, $u_{sh}(t)$ [U/day] is the shot input, and $u(t)$ is the input calculated by the control law. The initial injection dose $u_0 = 30[U]$ of insulin. On the following days, injection is calculated from the titration algorithm or control law, as seen in (15). Due to the injection shot being calculated form the previous day a delay is introduced into the system.

2.5 Biological Variability

Several sources of variance can affect the day-to-day variance of FG concentration of a T2D patient. These sources

include, but are not limited to, metabolic variability including insulin variability, variation due to lifestyle and adherence, and device-related variability (Aradóttir et al., 2017).

In (Ollerton et al., 1999), the day-to-day intraindividual variability of fasting plasma glucose in newly diagnosed, previously untreated individuals were monitored. Results found that 95% of the FG concentration of the group of subjects varied daily with $\sim$ 14% caused by biological variability. Hence the coeffcient of variation (CV) for fasting glucose is 14%. As the results are expressed in percentages, subjects with higher FG concentration were likely to experience more significant day-to-day variability.

In simulation, it is assumed that no insulin is omitted and biological variance is at its minimum, and no lifestyle or insulin adherence variability of FG concentration is present. Therefore based on the study mentioned above, a variance is added to simulated FG concentration by setting (Aradóttir et al., 2017),

$$\hat{FG}(k) = x_4(\lfloor t \rfloor) + v(k) \tag{16}$$

with $\lfloor \cdot \rfloor$ the rounding down operation, $k \in \mathbb{N}$ denoting day number, $t \in [k, k+1)$ and $v(k) \sim \mathcal{N}(0, (0.14 x_4(\lfloor t \rfloor))^2)$. Hence $\hat{FG}(k)$ represent simulated FG with biological variance as measurement noise. To simulate process uncertainty white noise, $v(j)$ is added to the model, in the simulation of patients. It is important to note that this noise is only added in simulation and is not accounted for in the derivation of the controller.

2.6 Rule-Based Titration Algorithm

As a benchmark for comparison with the LPV control strategy, the treat-to-target rule-based titration algorithm in (Aradóttir et al., 2017) is used. Given a specific starting dose, the patients adjust their insulin dose based on daily FG measurements, by various amounts depending on which FG interval their measurement lies within, see Table 3. Furthermore, dose adjustments are not performed in the first three days of simulation.

Table 3. Dose adjustments of the rule-based titration algorithm. Adjustments are based on the average FG of three day above target or the lowest below target (Aradóttir et al., 2017)

FG [mmol/l]	Dose adjustment
<3.1	-4U
3.1 - 3.9	-2U
4.0 - 5.0	In target: No change
5.1 - 7.0	+2U
7.1 - 8.0	+4U
8.1 - 9.0	+6U
>9.0	+8U

2.7 LPV Representation

Linear parameter-varying systems are parametrized linear dynamical systems whose mathematical description depends on parameters that change values over time.

The polytopic framework offers a simple and convenient way for representing and analyzing LPV systems. The general LPV system:

$$\begin{aligned} \dot{x}(t) &= A(\rho)x(t) + Bu(t) + Ew(t) \\ y(t) &= Cx(t) \end{aligned} \tag{17}$$

is represented as a convex combination of linear time-invariant systems:

$$\dot{x}(t) = \left(\sum_{i=1}^{2^N} \lambda_i(\rho) A_i \right) x(t) + Bu(t) + Ew(t) \tag{18}$$

$$y(t) = Cx(t) \tag{19}$$

where $x \in \mathbb{R}^n$ is the state of the system, $u \in \mathbb{R}^m$ is the control input to the system,$w \in \mathbb{R}^p$ is the exogenous input, $y \in \mathbb{R}^r$ is the measured output and N specify the number of parameters. The parameter vector $\rho \in \mathbb{R}^N$ is constrained by

$$\rho = [\rho_1(t), \rho_2(t), ..., \rho_N(t)] \in \Delta_N \tag{20}$$

where Δ_N is a bounded convex polytope (see (24)). To describe Δ_N let first the set $\boldsymbol{\rho}$ be defined by

$$\boldsymbol{\rho} = \left\{ \underline{\rho}_1, \overline{\rho}_1, ..., \underline{\rho}_N, \overline{\rho}_N \right\}, \quad \underline{\rho}_i < \overline{\rho}_i, \quad i = 1, ..., N$$

with $\overline{\rho}_i$ and $\underline{\rho}_i$ the upper and lower bound of parameter ρ_i, respectively. Secondly, for each pair $(i, j) \in \mathbb{N}^2$ define:

$$Q(i,j) = \left\lceil \frac{i}{2^{(j-1)}} \right\rceil \mod 2 \tag{21}$$

with $\lceil \cdot \rceil$ the rounding up operation, and mod the modulo operation. Finally for given $\boldsymbol{\rho}$ define the set of 2^N corner points

$$\mathscr{V}(\boldsymbol{\rho}) = \{v_1, ..., v_{2^N}\} \tag{22}$$

with $v_i \in \mathbb{R}^N$ and the j-th coordinate of v_i defined by

$$v_{ij} = \begin{cases} \overline{\rho}_j & \text{if } Q(i,j) = 0 \\ \underline{\rho}_j & \text{if } Q(i,j) = 1 \end{cases} \quad j = 1, ...N\,. \tag{23}$$

The constraining set Δ_N from (20) can then be defind by

$$\Delta_N = Co(\mathscr{V}(\boldsymbol{\rho})) \tag{24}$$

with $Co(S)$ the convex hull of the set S.

Now that Δ_N has been defined, $\lambda_i \colon \Delta_N \to \Lambda_N$ (with Λ_N the N-unit simplex), and A_i from Eq. (18) can be defined:

$$A_i = A(v_i) \tag{25}$$

$$\lambda_i(\rho) = \prod_{j=1}^{N} a_{ij}(\rho_j) \tag{26}$$

$$a_{ij}(\rho_j) = \begin{cases} \dfrac{\rho_j - \underline{\rho}_j}{\overline{\rho}_j - \underline{\rho}_j} & \text{if } Q(i,j) = 1 \\ \dfrac{\overline{\rho}_j - \rho_j}{\overline{\rho}_j - \underline{\rho}_j} & \text{if } Q(i,j) = 0 \end{cases}. \tag{27}$$

The left-hand side of (25) indicate that the entries of the $n \times n$ matrix $A(v_i)$ are functions of v_i, e.g., as $A_p = A_p(\bar{x}_4)$ in (13). Moreover, note that

$$\sum_{i=1}^{2^N} \lambda_i(\rho) = 1, \quad \lambda_i(\rho) > 0, \quad i = 1, ..., 2^N. \tag{28}$$

The general description above can now be applied to the physiological system studied here. The system (13) has a bilinear term in $\bar{x}_4$ coming from the matrix element $(A_p)_{43}$. By taking $\bar{x}_4$ in $(A_p)_{43}$ as a time-varying parameter ρ, the non-linearities can be hidden. That is,

$$A_p(\rho) = A_p(\bar{x}_4) \tag{29}$$

Table 4. Values obtained using the Matlab command `icdf` evaluated at $P \in \{0.05, 0.95\}$.

Parameter	Value (3 param.)	Value (4 param.)
$\bar{\rho}_1,\ \underline{\rho}_1$	1, 0	1, 0
$\bar{\rho}_2,\ \underline{\rho}_2$	54.3113, 23.8624	117.6617, 11.0146
$\bar{\rho}_3,\ \underline{\rho}_3$	3.3424, 1.6976	3.3424, 1.6976
$\bar{\rho}_4,\ \underline{\rho}_4$		0.6045, 0.2755

so

$$(A_p(\rho))_{43} = -\rho\frac{p_4}{p_3} \tag{30}$$

and all other matrix elements $(A_p(\rho))_{ij}$ are as in (13). Similarly the parameters p_d, p_4, p_7 (which are assumed constant for a specific patient) could potentially also be considered as time-varying parameters in an LPV model. Therefore in the sequel three scenarios will be considered; a one parameter $\rho = \bar{x}_4$, a three parameter $\rho = (\bar{x}_4, \frac{1}{p_d}, p_7)$, and a four parameter $\rho = (\bar{x}_4, \frac{1}{p_d}, p_7, p_4)$ LPV model. In the one and three parameter case the the model is affine in the parameters. In the four parameter case this is not the case due to the bilinear term in A_{43}. We therefore do an approximation by considering the system obtained as the convex hull of the corner matrices from (25). The upper and lower bounds for the parameters are as in Table 4.

3. CONTROLLER DESIGN

In this section, a dynamic-output feedback controller (DOF) on the form (31), which quadratically stabilises the LPV system (32) will be considered. The motivation is to derive a controller, which does not require the implementation of an observer. The general form of the control structure is

$$\begin{aligned} \dot{x}_c(t) &= A_c(\rho(t))x_c(t) + B_c(\rho(t))y(t) \\ u(t) &= C_c(\rho(t))x_c(t) + D_c(\rho(t))y(t) \end{aligned} \tag{31}$$

where $x_c \in \mathbb{R}^n$ is the controller state and $y \in \mathbb{R}^r$ is the measured output of the Generic Parameter Dependent System

$$\begin{aligned} \dot{x}(t) &= A(\rho(t))x(t) + B(\rho(t))u(t) + E(\rho(t))w(t) \\ z(t) &= C(\rho(t))x(t) + D(\rho(t))u(t) + F(\rho(t))w(t) \\ y(t) &= C_y(\rho(t))x(t) + F_y(\rho(t))w(t) \end{aligned} \tag{32}$$

with $x \in \mathbb{R}^n$ the systems states, $u \in \mathbb{R}^m$ the controlled input, $z \in \mathbb{R}^q$ the controlled output, and $w \in \mathbb{R}^p$ the exogenous input.

In this paper the controlled output $z(t)$ is designed as

$$z(t) = e(t) + \int_0^t e(s)ds + Du(t) \tag{33}$$

with $e(t) = r(t) - x_4(t)$ the error, $r(t) = r = 4.5\alpha$ the reference taken as the preferred glucose concentration in plasma (4.5 [mmol/l]) and leaving D as a tuning parameter. In summary the physiological system studied here can be represented by the LPV system

$$\begin{bmatrix} \dot{x} \\ \dot{x}_I \end{bmatrix} = \begin{bmatrix} A_p(\rho) & 0_{6\times1} \\ -C & 0_{1\times1} \end{bmatrix} \begin{bmatrix} x \\ x_I \end{bmatrix} + \begin{bmatrix} B_p \\ 0 \end{bmatrix} u + \begin{bmatrix} E_p & 0_{6\times1} \\ 0_{1\times1} & 1 \end{bmatrix} \begin{bmatrix} d_f \\ r \end{bmatrix} \tag{34}$$

$$z = [-C\ 1] \begin{bmatrix} x \\ x_I \end{bmatrix} + 0.05u + [0\ 1] \begin{bmatrix} d_f \\ r \end{bmatrix} \tag{35}$$

$$y = [-C\ 1] \begin{bmatrix} x \\ x_I \end{bmatrix} + [0\ 1] \begin{bmatrix} d_f \\ r \end{bmatrix} \tag{36}$$

and the dynamic-output feedback controller can be obtained by applying Theorem 3.3.4 and Proposition 3.3.5 from (Briat, 2014). In the one parameter case this yields

$$A_c(\rho) = A_{c0} + \rho A_{c\rho} \tag{37}$$

$$A_{c0} = \begin{bmatrix} -5.49 & -3.34 & -0.57 & 0.12 & -1 & -0.0004 & 0.008 \\ -7 & -12 & -2.08 & 0.44 & -3.6 & -0.0014 & 0.029 \\ -15.45 & 2.94 & -12.43 & -1.3 & 7.9 & -0.034 & 0.014 \\ 0.39 & -3.16 & -1.82 & -33.2 & -0.3 & -0.001 & -0.006 \\ 3.69 & 34.74 & 12.16 & -1.8 & -33 & 0.046 & 0.07 \\ 3705.02 & -526 & -772.4 & 26.16 & 171 & 3.23 & 2.37 \\ -171008 & 40989 & 20554 & -1918 & 13476 & -856.06 & -76.05 \end{bmatrix} \tag{38}$$

$$A_{c\rho} = \begin{bmatrix} 0.0005 & 0.0008 & -0.004 & 0.0002 & -0.0003 & 0.0001 & 0.000002 \\ 0.006 & 0.01 & -0.05 & 0.002 & -0.004 & 0.0007 & 0.00002 \\ 4.4 & 8.1 & -34.6 & 1.7 & -2.9 & 0.6 & 0.01 \\ -0.5 & -0.9 & 4.0 & -0.2 & 0.3 & -0.1 & -0.002 \\ 4.1 & 7.6 & -32.2 & 1.6 & -2.7 & 0.5 & 0.01 \\ 118.8 & 219.9 & -935.4 & 47.1 & -79.2 & 14.9 & 0.4 \\ 6825.9 & 12631.4 & -53729.8 & 2704.4 & -4551.9 & 856.4 & 22.6 \end{bmatrix} \tag{39}$$

$$B_c = \begin{bmatrix} -0.000003 \\ -0.00001 \\ -0.00002 \\ 0.000003 \\ -0.00003 \\ 0.005 \\ -0.227 \end{bmatrix}, \quad C_c = \begin{bmatrix} -18343451.1 \\ -21144114.6 \\ -4021526.5 \\ 862970.6 \\ -6965816.7 \\ -2698.7 \\ 56605.0 \end{bmatrix}^T \tag{40}$$

$$D_c = -20. \tag{41}$$

The three and four parameter case is obtained similar to the above. For comparison a PI controller $u(t) = D_c y(t)$, with the numerical value of D_c identical to the LPV case, will also be tested.

4. RESULTS

The results of regulating fasting glucose concentration in T2D with the Dynamic-Output Feedback controller, with 1, 3 and 4 time-varying parameters, the PI controller, and the rule-based titration algorithm, can be seen in

- **Case 1:** Fig. 2, 3, 4, and 5 respectively, when using the values from column two in Table 2.
- **Case 2:** Fig. 6, 7, 8, and 9 respectively, when using the values from the third column in Table 2 with $\sigma_4 = 0.01$ to simulate patients, $\sigma_4 = 0.1$ to calculate the control law, and p_7 as in column two. Note that the two choices of σ_4 implies that the control law is robust towards variations in p_4.

The two graphs in each of the figures are obtained by for each time instance to plot the maximum and minimum FG concentrations (with a CV of 14%) of the 810 (case 1) and 2480 (case 2) simulations. Moreover, an intensity plot (in blue) is superimposed on each of the figures illustrating the number of trajectories going through each point.

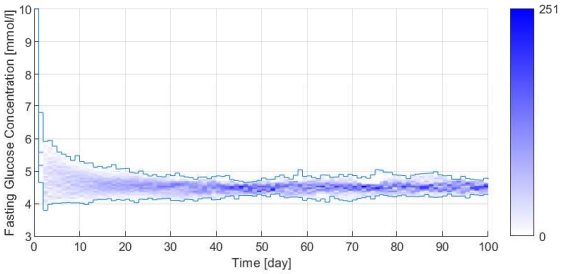

Fig. 2. Fasting glucose of T2D patients regulated by the Dynamic-Output Feedback control with 1 time varying parameter (case 1).

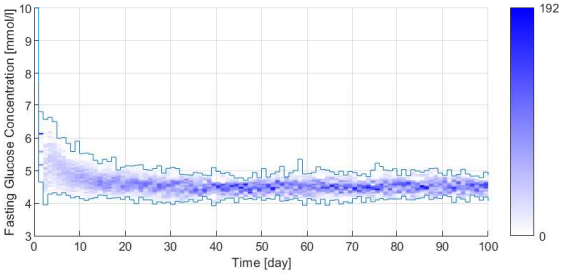

Fig. 3. Fasting glucose of T2D patients regulated by the Dynamic-Output Feedback control with 3 time varying parameters (case 1).

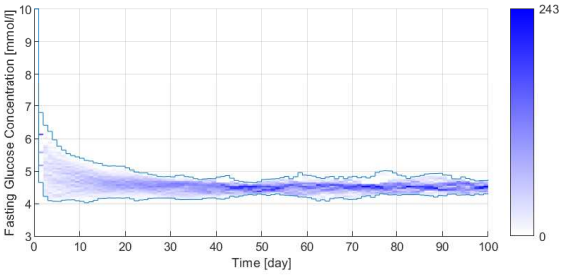

Fig. 4. Fasting glucose of T2D patients regulated by the PI control (case 1).

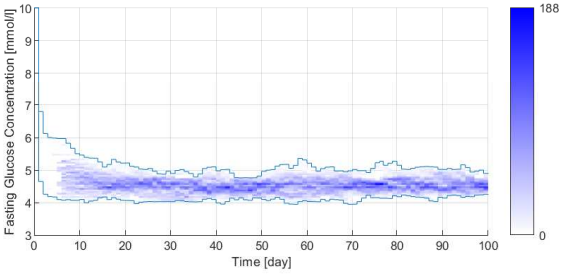

Fig. 5. Fasting glucose of T2D patients regulated by the Rule-based titration algorithm (case 1).

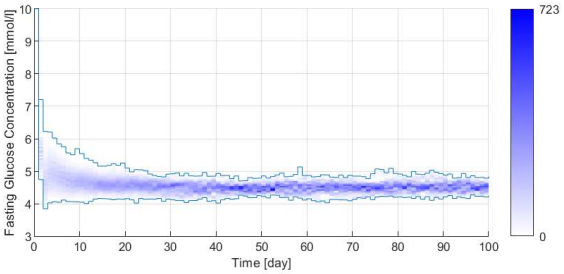

Fig. 6. Fasting glucose of T2D patients regulated by the Dynamic-Output Feedback control with 1 time varying parameter (case 2).

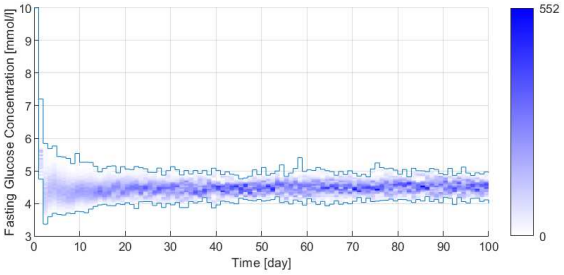

Fig. 7. Fasting glucose of T2D patients regulated by the Dynamic-Output Feedback control with 4 time varying parameters (case 2).

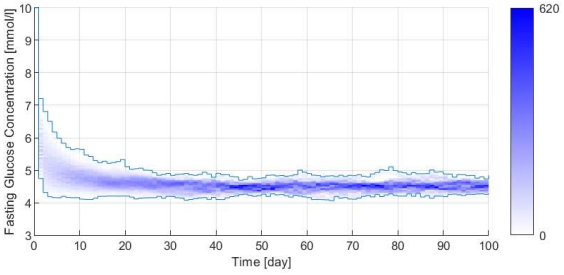

Fig. 8. Fasting glucose of T2D patients regulated by the PI control (case 2).

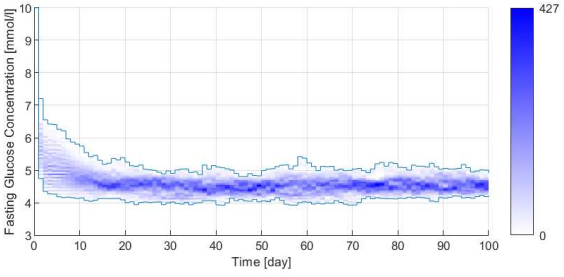

Fig. 9. Fasting glucose of T2D patients regulated by the Rule-based titration algorithm (case 2).

4.1 Comparison of methods

The four methods are compared by the settling time, variance and violations, shown in Table 5 and 6. The settling time

$$t_{p\%} = \max\{l = 1, 2, \ldots, p \mid t_{p\%,l}\},$$

with p=2430 or p=810 patients, denotes the maximum of the first time after which the lth output does not violate the 4 and 5 mmol/l bounds more than $p\%$ of the time during the time interval $[t_{p\%,l}, 100]$, with $t_{p\%,l}$ characterised by

$$p\% = \frac{\text{Total length of time intervals in } [t_{p\%,l}, 100] \text{ where } y^l(t) \notin [4, 5]}{100 - t_{p\%,l}}$$

with y^l denoting patient l. The variance $v_{p\%}$ is relative to $t_{p\%}$ and given by

$$v_{p\%} = \frac{1}{n} \sum_{i=1}^{p \cdot s(t_{p\%})} \left(s_i - \frac{1}{n} \sum_{j=1}^{p \cdot s(t_{p\%})} s_j \right)$$

with $s(t_{p\%})$ equal to the number of samples in $[t_{p\%}\ 100]$, and $s_k \in S_{t_{p\%}}$ with

$$S_{t_{p\%}} = \{y_1(t_{p\%}), y_1(t_{p\%} + 1), \ldots, y_1(100), y_2(t_{p\%}), \ldots \\ \ldots, y_p(t_{p\%}), y_p(t_{p\%} + 1), \ldots, y_p(100)\}$$

and $y^l(q)$ the q-sample output of patient l. That is, $v_{p\%}$ is the variance of the sample data $S_{t_{p\%}}$. The violations is the integrated amount of violations from the accepted interval as depicted in Fig 6.

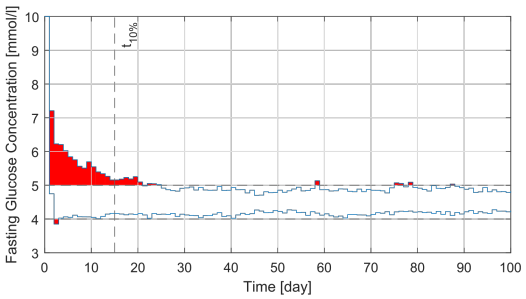

Fig. 10. Indication of the $t_{10\%} = 15$ settling time, and violation (=12.32) in red, related to Figure 6.

Table 5. Performance comparison between methods (DOF - Dynamic-Output Feedback 1 and 3 time-varying parameters, PI - standard PI controller, and R.B. - Rule Based Titration algorithm (Pfützner et al., 2016)

Case 1	CV 14%			
	DOF 1	DOF 3	PI	R.B.
$t_{10\%}$	10	14	15	67
$t_{20\%}$	1	1	4	8
$v_{10\%}$	0.023	0.034	0.019	0.032
$v_{20\%}$	0.343	0.37	0.039	0.044
Violations	8.583	16.523	10.703	16.795

Table 6. Performance comparison between methods (DOF - Dynamic-Output Feedback 1 and 4 time-varying parameters, PI - standard PI controller, and R.B. - Rule Based Titration algorithm (Pfützner et al., 2016)

Case 2	CV 14%			
	DOF 1	DOF 4	PI	R.B.
$t_{10\%}$	15	8	15	89
$t_{20\%}$	3	1	4	14
$v_{10\%}$	0.021	0.036	0.020	0.032
$v_{20\%}$	0.036	0.356	0.040	0.038
Violations	12.32	10.75	14.31	21.85

Case 1: Overall, the Dynamic-Output Feedback controller with 1 time-varying parameters performs better than the other methods with lowest settling times and violation, and a $v_{10\%}$ close to the lowest value which is obtained for the PI controller. The $v_{20\%}$ is high compared to the PI controller and the rule-based algorithm, however this is due to the small value of $t_{20\%}$. The Dynamic-Output Feedback controller with 3 time-varying parameter has better settling time performance compared to the PI controller and the rule-based algorithm, but is outperformed on variance and violations. The rule-based algorithm performs the worst overall. Note that there are close to zero hypoglycemia events.

Case 2: Overall, the Dynamic-Output Feedback controller with 4 time-varying parameters performs better than the other methods with lowest settling times and lowest violation. The Dynamic-Output Feedback controller with 1 time-varying parameter has a performance similar to the PI controller. However, the Dynamic-Output Feedback controller controller has a lower violation, coming from the faster convergence in the transient period. The rule-based algorithm performs the worst overall, as it only has a lower variance than the Dynamic-Output Feedback controller with 4 time-varying parameters. The possibility of hypoglycemia seen in Fig 7 can be removed by changing the reference value slightly. In this case performance of the Dynamic-Output Feedback controller with 4 time-varying parameters will be similar to the PI controller as seen in Fig. 11

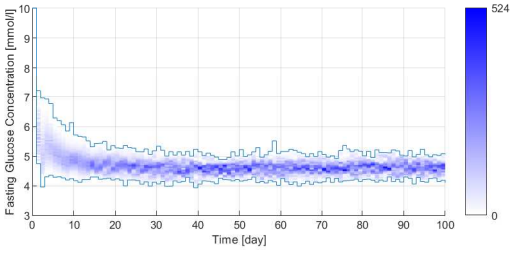

Fig. 11. Fasting glucose of T2D patients regulated by the DOF 4 control with reference at 4.6 [mmol/l]

5. CONCLUSION

Through simulation of T2D patients with the control methods, Dynamic-Output Feedback control, PI control, and the rule-based algorithm, it can be concluded that

the standard rule-based algorithm is outperformed by the other control methods, both in terms of settling time and violation of nominal fasting glucose concentration range. The Dynamic-output Feedback controller proved to overall have the best performance, with fast settling times and low violation. It is noted that the PI controller performed somewhat similar to the 3 parameter Dynamic-output Feedback controller in case 1, and to the 1 parameter Dynamic-output Feedback controller in case 2. Finally, it should be remarked that the Dynamic-Output Feedback and the PI controller concentrate trajectories around the reference value significantly better than the rule-based approach. This is indicated by the intensity (blue) in the figures. In case 2, it is seen that the Dynamic-Output Feedback controller and the PI controller obtain maximum intensity values of 723, 552 and 620, while the rule-based approach only obtain 427. In case 1, the Dynamic-Output Feedback controller with 1 parameter and the PI controller obtain intensity values of 251 and 243, while the rule-based approach only obtain 188. From a practical point of view, to get better results than a rule-based approach, implementing a simple PI controller, tuned by LPV methods, could be a solution. However, an LPV dynamic-output feedback controller will provide more robustness to variability, while still offering better performance, especially in the transient period. One should of course be aware of the possibility of hypoglycemia when using the LPV approach.

ACKNOWLEDGEMENTS

Thanks to Tinna B. Aradóttir for helpful discussions.

REFERENCES

(2012). Lpv identification of the glucose-insulin dynamics in type i diabetes. *IFAC Proceedings Volumes*, 45(16), 559–564.

Aradóttir, T.B., Boiroux, D., Bengtsson, H., Kildegaard, J., Orden, B.V., and Jørgensen, J.B. (2017). Model for simulating fasting glucose in type 2 diabetes and the effect of adherence to treatment. *IFAC-PapersOnLine*, 50, 15086–15091. doi:10.1016/j.ifacol.2017.08.2527.

Aradóttir, T.B., Boiroux, D., Bengtsson, H., and Poulsen, N.K. (2018). Modelling of glucose-insulin dynamics from sparse data. *40th International Conference of the IEEE Engineering in Medicine and Biology Society*, 2354–2357. doi:10.1109/EMBC.2018.8512792.

Bolder, U., Ebener, C., Hauner, H., Jauch, K.W., Kreymann, G., Ockenga, J., Traeger, K., and group for developing the guidelines for parenteral nutrition of The German Association for Nutritional Medicine, W. (2009). Carbohydrates – guidelines on parenteral nutrition, chapter 5.

Briat, C. (2014). *Linear parameter-varying and time-delay systems*, volume 3. Springer.

Colmegna, P. and Peña, R.S.S. (2014). Linear parameter-varying control to minimize risks in type 1 diabetes. *IFAC Proceedings*, 47, 9253–9257.

Colmegna, P.H., Sanchez-Pena, R.S., Gondhalekar, R., Dassau, E., and Doyle, F.J. (2016). Switched lpv glucose control in type 1 diabetes. *IEEE Transactions on Biomedical Engineering*, 63(6), 1192–1200.

Diabetes.co.uk (2019). Blood sugar level ranges. URL `https://www.diabetes.co.uk/diabetes_care/blood-sugar-level-ranges.html`. Last accessed on 4-03-2020.

Eigner, G., Siket, M., Szakál, A., Rudas, I., and Kovács, L. (2018). Discrete lpv modeling of diabetes mellitus for control purposes. In *2018 IEEE International Conference on Systems, Man, and Cybernetics (SMC)*, 2558–2563. IEEE.

Hovorka, R. et al. (2004). Nonlinear model predictive control of glucose concentration in subjects with type 1 diabetes. *Physiological Measurement*, 25(4), 905–920.

International Diabetes Federation (2017). Idf diabetes atlas 8th edition.

Kanderian, S.S., Weinzimer, S., Voskanyan, G., and Steil, G.M. (2009). Identification of intraday metabolic profiles during closed-loop glucose control in individuals with type 1 diabetes. *Physiological Measurement*, 3(5), 1047–1057.

Löfberg, J. (2004). Yalmip : A toolbox for modeling and optimization in matlab. In *In Proceedings of the CACSD Conference*. Taipei, Taiwan.

Ollerton, R.L., Playle, R., Ahmed, K., Dunstan, F.D., Luzio, S.D., and Owens, D.R. (1999). Day-to-day variability of fasting plasma glucose in newly diagnosed type 2 diabetic subjects. *Diabetes care*, 22(3), 394–398.

Pfützner, A., Stratmann, B., Funke, K., Pohlmeier, H., Rose, L., Sieber, J., Flacke, F., and Tschoepe, D. (2016). Real-world data collection regarding titration algorithms for insulin glargine in patients with type 2 diabetes mellitus. *Journal of Diabetes Science and Technology*, 10, 1122–1129. doi:10.1177/1932296816654714.

Swigert, T.J. (2014). Basal insulin titration: Looking beyong the fasting glucose. *AADE in Practice*, 2, 34–40.

Wilinska, M.E., Chassin, L.J., Acerini, C.L., Allen, J.M., Dunger, D.B., and Hovorka, R. (2010). Simulation environment to evaluate closed-loop insulin delivery systems in type 1 diabetes. *Journal of diabetes science and technology*, 4(1), 132–144.